

# A lithospheric instability origin for Columbia River flood basalts and Wallowa Mountains uplift in northeast Oregon

T. C. Hales<sup>1</sup>, D. L. Abt<sup>1</sup>†, E. D. Humphreys<sup>1</sup> & J. J. Roering<sup>1</sup>

Flood basalts appear to form during the initiation of hotspot magmatism. The Columbia River basalts (CRB) represent the largest volume of flood basalts associated with the Yellowstone hotspot, yet their source appears to be in the vicinity of the Wallowa Mountains<sup>1</sup>, about 500 km north of the projected hotspot track. These mountains are composed of a large granitic pluton intruded into a region of oceanic lithosphere affinity<sup>2</sup>. The elevation of the interface between Columbia River basalts and other geological formations indicates that mild pre-eruptive subsidence took place in the Wallowa Mountains, followed by syn-eruptive uplift of several hundred metres and a long-term uplift of about 2 km. The mapped surface uplift mimics regional topography, with the Wallowa Mountains in the centre of a 'bull's eye' pattern of valleys and low-elevation mountains. Here we present the seismic velocity structure of the mantle underlying this region and erosion-corrected elevation maps of lava flows, and show that an area of reduced mantle melt content coincides with the 200-km-wide topographic uplift. We conclude that convective downwelling and detachment of a compositionally dense plutonic root can explain the timing and magnitude of Columbia River basalt magmatism, as well as the surface uplift and existence of the observed melt-depleted mantle.

The Yellowstone hotspot initiated ~17 Myr ago with a rapid succession of large eruptions starting at the McDermitt caldera in northern Nevada and propagating ~500 km north along the western edge of the Precambrian continental margin, first to Steens Mountains area in southeast Oregon and then to the site of the CRB eruptions in northeast Oregon<sup>1</sup> (Fig. 1). The total volume of erupted flood basalt is ~234,000 km<sup>3</sup>, 75% of which is CRB (ref. 3). The large geographic extent involved in these eruptions has been difficult to reconcile with a traditional plume model because nearly all flood basalt erupted north of the projected hotspot track, which trends from Yellowstone to the McDermitt caldera. Furthermore, the Snake River plain is a well-developed hotspot track, but it leads away from the CRB source area and arcs across the state of Idaho like a smile (Fig. 1 inset). Two recent suggestions accounting for the distributed and largely off-track nature of hotspot initiation modify the plume hypothesis by having plume impingement beneath either the Steens Mountains<sup>1</sup> or the central Idaho craton<sup>4</sup> and then flattening rapidly along a trend near the Precambrian continental margin. These plume models are supported by the presence of high <sup>3</sup>He/<sup>4</sup>He in the flood basalts<sup>5</sup>. In contrast, other models suggest that flood basalt magmatism represents passive back-arc processes<sup>6</sup>.

At present, little deformation occurs in northeast Oregon. Global Positioning System (GPS) and geologic data indicate clockwise rotation of much of Oregon relative to North America about a

pole near the bend in the Precambrian continental margin (Fig. 1), consistent with regional tectonics<sup>7,8</sup>. E–W extension on normal faults occurs with increasing rate south of this location, and N–S contraction, expressed as E–W-oriented folds, is increasingly active to the west. This regional tectonic setting has persisted since eruption of the CRB without noticeable change<sup>7,9</sup>, and proximity to the pole implies very low deformation rates for northeast Oregon. The regional ~N–S axis of maximum compression<sup>9–12</sup> responsible for these faults and folds was also responsible for the NNW–SSE trending Chief Joseph dike swarm, E–W folds such as the Lewiston anticline and NW–SE-oriented strike-slip structures such as the Olympic–Wallowa Lineament<sup>10–12</sup>. Some young structures near the Wallowa Mountains have deformed in an exceptional manner that is inconsistent with the regional stress field. These include the WNW–ESE-oriented Wallowa normal fault, the oblique normal Limekiln and Hite Fault systems and the NE–SW-oriented folds such as the Troy basin syncline<sup>12</sup>. We suggest that these inconsistencies with the regional stress field represent local perturbations that may be caused by local contrasts in strength or buoyancy.

CRB lavas erupted onto a low-relief surface of Mesozoic accreted ocean terranes stitched together by Jurassic plutons, of which the Wallowa pluton is the largest<sup>13</sup> (Fig. 1). After initial Imnaha flows filled the valleys, subsequent eruptions deposited thin, flat-lying sheets that provide a useful datum to measure deformation accurately. These flows are found in Hells Canyon at an elevation of 1,100 m and atop the Wallowa Mountains at 2,700 m, demonstrating substantial vertical motion following their eruption<sup>14</sup>. Grande Ronde eruptions followed the Imnaha, depositing about 80% of the CRB lavas over ~1 Myr. We correct elevation maps of the Grande Ronde magnetostratigraphic units (which are subdivided into R<sub>1</sub>, N<sub>1</sub>, R<sub>2</sub> and N<sub>2</sub> units)<sup>14–16</sup> for the effects of erosional unloading<sup>17,18</sup> to obtain markers of post-eruptive deformation (Fig. 2, Supplementary Figure S1). The uplift and downwarp of these flows closely conform to current topography, with up to 2 km of uplift focused on the Wallowa pluton (Figs 1 and 2) and more subdued uplift centred on the lesser plutons in the area (Fig. 1). The history of Imnaha and Grande Ronde uplift reveals the early evolution of local buoyancy. Imnaha basalts ponded in incipient basins, indicating possible pre-eruptive subsidence<sup>19</sup>. Basin development continued during Grande Ronde eruptions, causing local ponding and thickening of flows, while syn-eruptive uplift created locally thinned units. In particular, ~300 m of uplift resulted in a thinned N<sub>2</sub> unit near its source close to the Wallowa Mountains<sup>19,20</sup> (Supplementary Fig. S1). Post-Grande-Ronde deformation is evidenced by the contrasting distributions of Grande Ronde and late CRB Wanapum (15–14 Myr ago) and Saddle Mountains (14–6 Myr ago) flows, which show distinctive,

<sup>1</sup>Department of Geological Sciences, 1272 University of Oregon, Eugene, Oregon 97403, USA. †Present address: Department of Geological Sciences, Brown University, 324 Brook Street, Providence, Rhode Island 02912, USA.

well-developed channelization and ponding in response to emerging topographic relief<sup>21</sup>. Significant relief generation occurred at 14.5–13 Myr ago, coincident with initiation of the La Grande, Baker and Weiser grabens, which surround the Wallowa Mountains<sup>19</sup>. This structural evidence leads us to conclude that most Wallowa Mountains uplift occurred in <10 Myr (Fig. 2c).

The current physical state of the upper mantle provides a constraint on the origin of buoyancy. We obtain a basic assessment of upper mantle structure by tomographically inverting ~600 teleseismic P-wave delays collected by a six-station array of IRIS-PASSCAL seismometers deployed in the region. Relatively high-velocity mantle is imaged beneath the bull's eye region (Fig. 3). Resolution 'squeezing' tests<sup>22</sup> (Fig. 3b) indicate that this seismically fast volume extends from ~75 km to at most a depth of 175 km, and its horizontal extent is coincident with the bull's eye pattern (Fig. 3). The occurrence of basaltic volcanism in the recent past and the major uplift in the Wallowa Mountains are inconsistent with the high-velocity mantle being relatively cool. The only reasonable alternative is that melt content has been reduced (and possibly eliminated) by eruption of the CRB from the high-velocity volume<sup>22,23</sup>. This hypothesis is strengthened by the spatial correlation between the upper mantle high-velocity volume and the location of flood basalt dykes (Figs 1 and 3). The implied mantle depletion would increase mantle buoyancy by an amount that accounts for the observed several hundred metres of syn-eruptive uplift<sup>24</sup>. Using the equations of Schutt and Leshner<sup>24</sup>, a simple calculation suggests that 5% depletion of an 80-km-thick layer (for example, 70–150 km) would

cause ~300 m of isostatic uplift in the region. However, mantle basalt depletion cannot account for the focused ~2 km of surface uplift of the Wallowa Mountains.

The unusual tectonic and magmatic history of northeast Oregon has similarities to two recently studied events that involve apparent small-scale convective instability driven by dense garnet-rich crust and mantle lithosphere. Elkins-Tanton and Hager<sup>25</sup> account for pre-eruptive subsidence of the Siberian traps flood basalts with the initial downwelling of dense eclogitic lower lithosphere beneath the area of downwarping, and attribute the magmatism to decompression melting of ascending asthenosphere flowing into the vacated regions. Saleeby and Foster<sup>26</sup> compile abundant evidence for young and ongoing convective descent (termed 'delamination' in their paper) of the garnet-rich rocks that are the genetic complement to the granitic Sierra Nevada pluton in California. As this dense lower crust and upper mantle sinks, the overlying southern Sierra Nevada Mountains rise in isostatic response.

In northeast Oregon, where granitic plutons are scarce, major uplift is concentrated on the largest pluton in the region. We attribute this uplift to the convective removal of the pluton's dense roots, and consider the magnitude of uplift and its strong association with the Wallowa pluton difficult to account for with any other process. Furthermore, such a delamination-driven model can also explain the remarkable bull's eye uplift pattern, the post-eruptive timing of most uplift, and the associated CRB outpourings. We envision initial convective instability of the plutonic roots creating a drip-like downwelling that pulls the Wallowa region down, creating

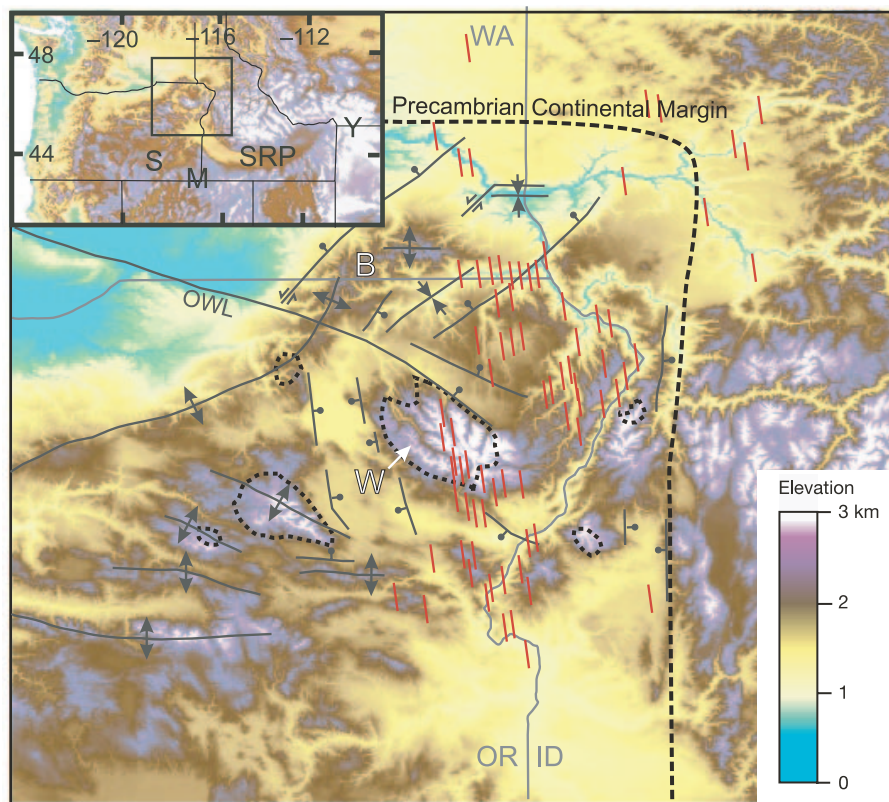


**Figure 1 | Regional structural and location maps for northeast Oregon.** Location map showing CRB source area, the Wallowa (W) and Blue (B) Mountains. Productive Grande Ronde dikes are shown as short red lines drawn in the average orientation of these features. These dykes show the approximate location of major dykes and the line length does not represent the actual length of dykes<sup>1</sup>. Major extensional (lines with balls) and contractional (lines with double-headed arrows) structures are indicated<sup>12</sup>. The Precambrian continental margin, represented with  $^{87}\text{Sr}/^{86}\text{Sr} = 0.706$  in areas where it is not exposed, is indicated with a dashed line. Major plutons

west of Precambrian North America are outlined with heavy dotted lines. WA, Washington; OR, Oregon; ID, Idaho; OWL, Olympic-Wallowa Lineament. Inset, map of the western United States showing locations of major magmatic centres in relation to the Yellowstone hotspot, including: the McDermitt caldera (M), the Steens Mountains (S) and the source of the CRB eruptions in northeast Oregon (small rectangle). The arcuate Snake River Plain (SRP) is the Yellowstone hotspot track leading to the active Yellowstone caldera (Y). US State boundaries are shown as solid lines. Note the bull's eye pattern of uplift at the northwest end of the SRP.

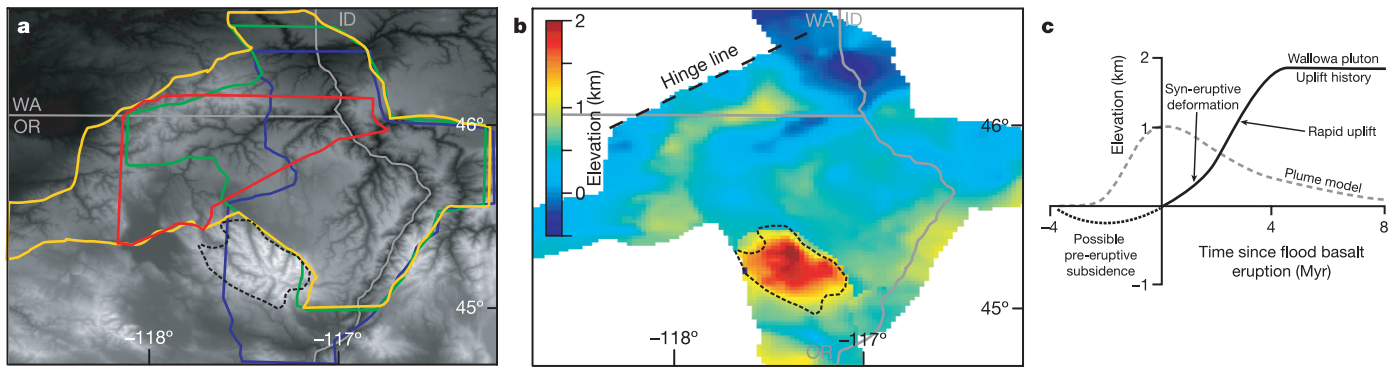


**Figure 2 | Maps of post-eruptive uplift in the Wallowa Mountains area.** **a**, Digital elevation map showing the overlapping distribution of exposed Grande Ronde magmatostratigraphic interfaces used for analysis of Wallowa Mountains uplift: Imnaha-R1 (blue), R1-N1 (green), N1-R2 (yellow) and R2-N2 (red). **b**, Composite surface for Grande Ronde uplift. This surface was made by vertically shifting the individual interfaces using published flow thicknesses<sup>14</sup>, smoothing the resulting surface with a mild low-pass filter, and removing the effects of erosional unloading by deconvolving the point load response of an elastic plate<sup>17,18</sup>, assuming total coverage by the Grande Ronde lavas and an elastic thickness of 5 km, similar to other estimates from this area<sup>22</sup>. The absolute elevation is referenced to a hinge line (dotted black line) that separates the uplifted Blue Mountains from the down-dropped Pasco basin immediately northwest of the Blue Mountains. **c**, Schematic plot

pre-eruptive subsidence (Fig. 2c). Asthenosphere flowing up into the area around the Wallowa downwelling decompresses and partly melts upon ascent, creating initial CRB flows that pond in the depression. As the dense mantle and lower crust sink and detach from the lithosphere, surface uplift begins and magmatism accelerates within the circular area where decompression melting is excited. The uplift of  $\sim 300$  m that occurred during this time interval is controlled by the combined effects of melt accumulation in magma chambers and chamber evacuation, and residual buoyancy created by basalt depletion. Finally, continued sinking of the dense Wallowa pluton root causes continued uplift of the Wallowa pluton, which progresses until the sinking mass is effectively

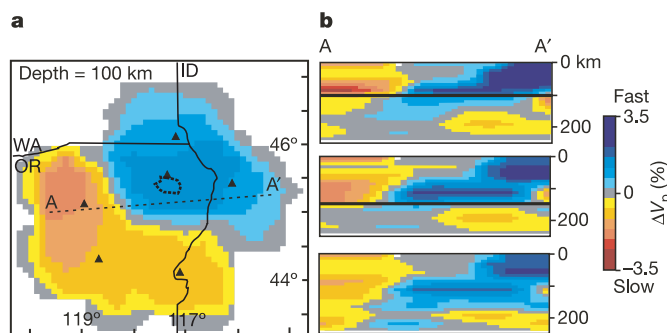


**Figure 3 | Tomographic images of northeast Oregon.** **a**, Upper mantle P-wave velocity variations at 100 km depth, imaged by teleseismic tomography from data recorded by six seismometers (triangles). Also shown is the Wallowa pluton (dotted line) and cross-section location (dashed line). **b**, Cross-sections through 'squeezed' inversions. These are hypothesis tests in which we found the structure that best accounts for the observed delays and that is confined above the black line; after relaxing the depth constraint, creation of significant structure below the black line indicates that deeper structure is required. The upper cross-section (squeezing depth = 100 km) indicates a strong need for structure below 100 km. The middle panel (squeezing depth = 150 km, and used for **a**), like the lower (unconstrained) panel, indicates no need for high-velocity structure below a depth of 150 km. Imaging places the top of the high-velocity body near 75 km.  $\Delta V_p$  represents the percentage difference from average P-wave velocity.

of the Wallowa Mountains uplift history (dark line) and a hypothetical area affected by a thermal plume (grey line). Wallowa Mountain uplift history is controlled at three times. Pre-eruptive subsidence, inferred from ponding of early Imnaha lava flows in basins, is interpreted as the initiation of delamination. We calculated  $\sim 300$  m of syn-eruptive uplift in this area over the 1-Myr duration of the Grande Ronde eruption. This is followed by rapid uplift of the Wallowa Mountains 3–4 Myr after initial Imnaha eruption, indicated by the development of structures bounding the Wallowa Mountains<sup>14</sup>, and current topographic relief of the composite surface shown in **b**. We note that the hypothetical uplift curve for a thermal plume can vary significantly in magnitude, so we have chosen a representative amount of uplift predicted by CRB magmatism.

removed from the region and uplift becomes fully isostatic (Fig. 2c).

This model for flood basalt volcanism driven by delamination of compositionally dense roots has some interesting implications for Yellowstone hotspot initiation. We discuss two interpretations: First, if a plume impacted to the south of the CRB source area and propagated north along the Precambrian continental margin<sup>1,4</sup>, associated hot mantle material could trigger convective lithospheric instability of the Wallowa plutonic roots. This mechanism could thus provide a way of accounting for the intense magmatism far from the Yellowstone hotspot track. In this case, a significant modification to the plume hypothesis is not required and the problem of CRB magmatism is addressed. Second, the sequence of eruptions initiating the Yellowstone hotspot could have been caused by a series of delamination events, perhaps one triggering the next or all triggered by unusual back-arc activity, with no requirement for an active plume. In this case, magmatism could be related to a swath of fertile mantle lithosphere adjacent to the infertile Precambrian lithosphere that was recently hydrated in a fore-arc setting. In either case, delamination is required to initiate flood basalt volcanism in northeast Oregon, and we have shown there to be an intimate relationship between crustal structure and flood basalt initiation.

Received 14 March; accepted 6 October 2005.

1. Camp, V. E. & Ross, M. E. Mantle dynamics and genesis of mafic magmatism in the intermontane Pacific Northwest. *J. Geophys. Res.* 109, doi:10.1029/2003JB002838 (2004).
2. Lallemand, H. G. A. Pre-Cretaceous tectonic evolution of the Blue Mountains province, northeastern Oregon. *USGS Prof. Pap.* 1438, 271–304 (1994).
3. Camp, V. E., Ross, M. E. & Hanson, W. E. Genesis of flood basalts and basin and range volcanic rocks from Steens Mountain to the Malheur River Gorge, Oregon. *Geol. Soc. Am. Bull.* 115, 105–128 (2003).
4. Jordan, B. T. in *Plumes, Plates and Paradigms* (eds Foulger, G. R., Natland, J. H., Presnall, D. C. & Anderson, D. L.) 503–515 (Geological Society of America Memoir 388, Boulder, Colorado, 2005).
5. Dodson, A., Kennedy, M. B. & De Paolo, D. J. Helium and neon isotopes in the Imnaha Basalt, CRBG, evidence for a Yellowstone plume source. *Earth Planet. Sci. Lett.* 150, 443–451 (1997).
6. Anderson, D. L. The sublithospheric mantle as the source of continental flood basalts; the case against the continental lithosphere and plume head reservoirs. *Earth Planet. Sci. Lett.* 123, 269–280 (1994).



7. Wells, R. E., Weaver, C. S. & Blakely, R. J. Fore-arc migration in Cascadia and its neotectonic significance. *Geology* **26**, 759–762 (1998).
8. McCaffrey, R. *et al.* Rotation and plate locking at the southern Cascadia subduction zone. *Geophys. Res. Lett.* **27**, 3117–3120 (2000).
9. Hooper, P. R. The Columbia River flood basalt province: current status. *Geophys. Monogr.* **100**, 1–27 (1997).
10. Hooper, P. R. & Camp, V. E. Deformation of the southeast part of the Columbia plateau. *Geology* **9**, 323–328 (1981).
11. Camp, V. E. & Hooper, P. R. Geologic studies of the Columbia Plateau. Part 1. Late Cenozoic evolution of the southeastern part of the Columbia River basalt province. *Geol. Soc. Am. Bull.* **92**, 659–668 (1981).
12. Hooper, P. R. & Conrey, R. M. A model for the tectonic setting of the Columbia River basalt eruptions. *Geol. Soc. Am. (Spec. Pap.)* **239**, 293–306 (1989).
13. Goles, G. G. Miocene basalts of the Blue Mountains province in Oregon. I. Compositional types and their geological settings. *J. Petrol.* **27**, 495–520 (1986).
14. Walker, G. W. *Reconnaissance Geologic Map of the Oregon Part of the Grangeville Quadrangle, Baker, Union, Umatilla, and Wallowa Counties, Oregon Map* (USGS Misc. Investigations Series I-1116, 1979).
15. Reidel, S. P., Hooper, P. R., Webster, G. D. & Camp, V. E. *Geologic Map of Southeastern Asotin County, Washington* (Washington Division of Geology and Earth Resources Map Series, GM-40, 1992).
16. Hooper, P. R., Webster, G. D. & Camp, V. E. *Geologic Map of the Clarkson 15 Minute Quadrangle, Idaho and Washington* (Washington Division of Geology and Earth Resources Map Series GM-31, 1985).
17. Lambeck, K. *Geophysical Geodesy: the Slow Deformations of the Earth* Ch. 10 (Clarendon, Oxford, 1988).
18. Anderson, R. S. Evolution of the Santa Cruz Mountains, California, through tectonic growth and geomorphic decay. *J. Geophys. Res.* **99**, 20161–20179 (1994).
19. Camp, V. E. Geologic studies of the Columbia Plateau: Part II. Upper Miocene basalt distribution, reflecting source locations, tectonism, and drainage history in the Clearwater embayment Idaho. *Geol. Soc. Am. Bull.* **92**, 669–678 (1981).
20. Reidel, S. P. *et al.* The Grande Ronde Basalt, Columbia River Basalt Group; Stratigraphic descriptions and correlations in Washington, Oregon, and Idaho. *Geol. Soc. Am. (Spec. Pap.)* **239**, 21–54 (1989).
21. Tolan, T. L. *et al.* Revisions to the estimates of the areal extent and volume of the Columbia River Basalt Group. *Geol. Soc. Am. (Spec. Pap.)* **239**, 1–20 (1989).
22. Saltzer, R. L. & Humphreys, E. D. Upper mantle P-wave structure of the eastern Snake River Plain and its relationship to geodynamic models of the region. *J. Geophys. Res.* **102**, 11829–11841 (1997).
23. Hammond, W. C. & Humphreys, E. D. Upper mantle seismic wave velocity: The effect of realistic partial melt geometries. *J. Geophys. Res.* **105**, 10975–10999 (2000).
24. Schutt, D. L. & Leshner, C. E. The effect and seismic velocity of garnet and spinel lherzolite. *J. Geophys. Res.* (in the press).
25. Elkins-Tanton, L. T. & Hager, B. H. Melt intrusion as a trigger for lithospheric foundering and the eruption of the Siberian flood basalts. *Geophys. Res. Lett.* **27**, 3937–3940 (2000).
26. Saleeby, J. B. & Foster, Z. Topographic response to mantle lithosphere removal in the southern Sierra Nevada region, California. *Geology* **32**, 245–248 (2004).
27. Armstrong, R. L., Taubeneck, W. H. & Hales, P. O. Rb-Sr and K-Ar geochronometry of Mesozoic granitic rocks and their Sr isotopic composition, Oregon, Washington and Idaho. *Geol. Soc. Am. Bull.* **88**, 387–411 (1977).

**Supplementary Information** is linked to the online version of the paper at [www.nature.com/nature](http://www.nature.com/nature).

**Acknowledgements** We thank G. Goles for initial conversations regarding this manuscript. Funding for this work provided by National Science Foundation grants to J.J.R. and E.D.H. A review from M. Richards improved the manuscript. We thank J. Riker, D. Clippinger, C. Simmons and M. Giba for field assistance. We also thank N. Fay and J. Crosswhite for help with numerical analysis.

**Author Information** Reprints and permissions information is available at [npg.nature.com/reprintsandpermissions](http://npg.nature.com/reprintsandpermissions). The authors declare no competing financial interests. Correspondence and requests for materials should be addressed to T.H. ([thales@uoregon.edu](mailto:thales@uoregon.edu)).